

High resolution displacement detection by speckle pattern analysis : accuracy limits in linear displacement speckle metrology

Robert Filter
robert.filter@ds.mpg.de

Max-Planck-Institut für Dynamik und Selbstorganisation, Bunsenstr. 10, 37073 Göttingen, Germany

Toralf Scharf

Ecole Polytechnique Fédérale de Lausanne, EPFL - IMT - OPT, Rue A.-L. Breguet 2, 2000 Neuchâtel, Switzerland

Hans Peter Herzig

Ecole Polytechnique Fédérale de Lausanne, EPFL - IMT - OPT, Rue A.-L. Breguet 2, 2000 Neuchâtel, Switzerland

We propose a simple reflection measurement setup and a motion evaluation procedure based on a two dimensional recording of subsequent speckle images. The averaging of cross correlation functions is used to measure displacements. We demonstrate experimentally a 10 nm precision on a 50 μm measurement range limited by systematical errors. An image library is proposed to extend the measurement range. Limitations are given and documented improvements predicted an accuracy better than 5 nm over a range of 150 μm . [DOI: 10.2971/jeos.2010.10035S]

Keywords: inear displacement, speckles, non-contact measurements, laser measurements, optical sensing and sensors

1 INTRODUCTION

If a laser beam illuminates a rough surface, which has a surface roughness larger than the wavelength, the resulting intensity distribution shows a particular granular structure (speckle pattern). This phenomenon is well known and can be explained with classical methods of statistical optics [1, 2]. Whereas the speckle pattern might be a major drawback for many applications, it can be used in several ways as motion or vibration detector. An outstanding and successful end costumer application is the state-of-the-art computer mouse. In such devices, a lateral relative translation resolution of 5000 dpi or 5 μm is obtained by observing the speckle fields and applying specific signal processing [3]. These values have to be compared to industrially available absolute position encoders reaching 25000 dpi, i.e. 1 μm resolution [4] based on magnetic transducers or 50000 dpi (500 nm) with optical methods [5]. Such results are only possible by using averaging on a multisensor arrangement. To be more precise in the measurement would require the recording of finer structures.

If optical sensing is used, the smallest structure size that can be sensed with conventional optics, is given by the diffraction limit of the optical system, mainly determined by the wavelength of light and the numerical aperture. Because of the diffraction limited nature of the statistical light field in speckles, one can expect to achieve very accurate measurements of surface displacements. Theoretical calculations and measurements are given for instance in [6]. Since then, a lot of experiments were done using speckle metrology for displacement measurements. To the best of our knowledge and surprisingly, a resolution smaller than a tenth of a micrometer was not demonstrated experimentally in classical reflection setups. In [7], an accuracy of 0.1 μm without magnification optics is predicted. By measuring the position of optical

vortices an accuracy of 20 nm was achieved in [8] using white light and a magnification of 20 times. The position could only be extracted with computationally expensive analysis.

In this work, we present a simple setup to achieve accuracies better than 10 nm over a range of 50 μm . The range can be extended via an image library as will be shown in the following. The limitations will be pointed out, as well as future improvements.

2 MEASUREMENT PRINCIPLE

Figure 1 shows the measurement principle. A laser beam illuminates a rough surface which moves in one direction. The diffused light is observed in specular reflection by an objective lens. A detector array records the appearing speckle pattern. For small displacements, the speckle pattern follows linearly the motion as shown in [6]. The displacement of a discrete one-dimensional signal A can be measured in general by evaluating the shift of the peak of the cross correlation R between A and the displaced signal B . The cross correlation R can be expressed as

$$R(A, B; L) = \sum_k A(k) * B(k + L). \quad (1)$$

The calculation of the peak shift can be done via Gaussian interpolation. Since the motion goes in one direction only, it would be sufficient to measure the displacement with respect to a fixed signal with a single line detector array. A two dimensional detector array like a charged coupled device (CCD) can be seen as an ensemble of a large number of line detectors. This offers the possibility of statistically evaluating the

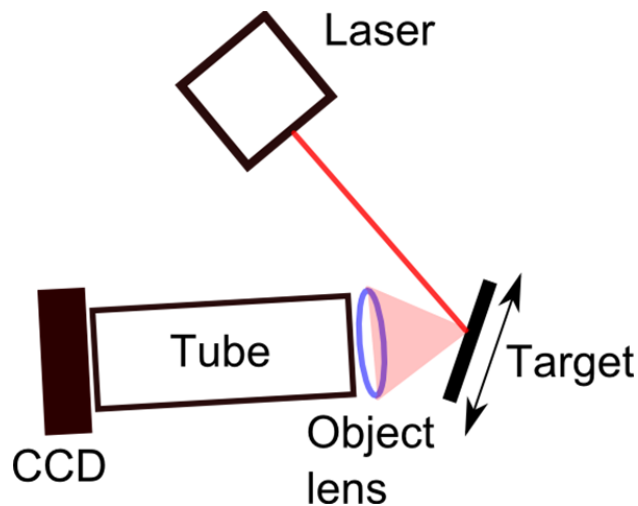


FIG. 1 Functional principle of the measurement system. A laser beam points on a diffusing surface. A camera positioned in specular reflection records subjective speckle images from the magnified image of the surface. The test surface can be moved with high precision. The magnification allows to increase the sensitivity to lateral displacements.

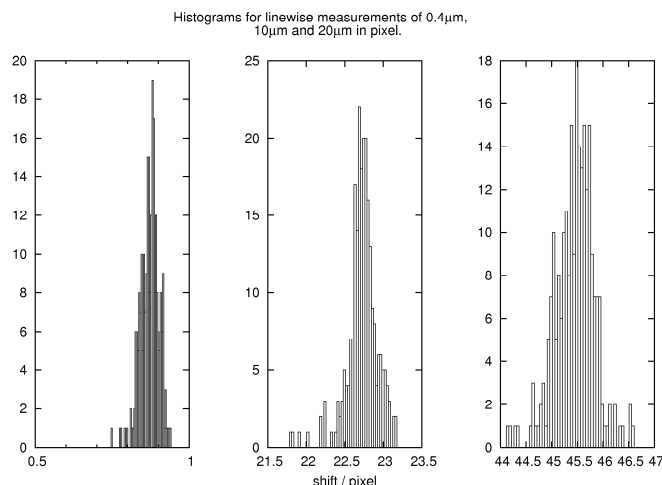


FIG. 2 Histograms of line wise measurements of different shifts for an experiment with a magnification of $m = 5$ and a CCD resolution of 1280×1024 pixels. The variance gets larger for longer shifts and the peak's distribution can be assumed to be Gaussian.

results obtained for each line, hence providing an increased accuracy. In our approach the displacements of the surface were calculated by line wise evaluation of the displacements with respect to a reference image and afterwards the data were fitted with a Gaussian bell curve. The center of this bell curve is taken as the displacement value. For small displacements the assumption of a bell curve is justified. Three typical histograms for different shifts with low magnification can be seen in Figure 2 for displacements of 0.4, 10 and 20 μm, respectively. With longer distance, the variance of the line wise measured positions increases caused by decorrelation. However, we observed that there is only a very small difference between calculating the line wise achieved displacements and fitting these data, or adding up the line wise cross correlations and fitting the resulting peaked data. One can also use this approach to save computing time, if it is sure that this variation of the method is justified.

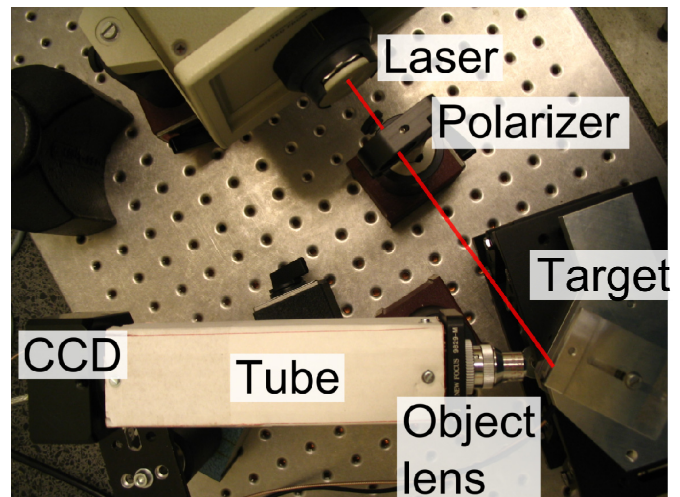


FIG. 3 Experimental setup. A stabilized laser beam (with a polarizer) illuminates an aluminum target-surface, which is mounted on a piezoelectrically driven table. The combination of the object lens and tube length realizes a magnification of about $m = 25$ on the CCD camera.

3 EXPERIMENTAL SETUP AND SPECKLE IMAGES

The measurement principle has been realized in the setup illustrated in Figure 3. The piezoelectrically driven stage is a P-762.1L from Physik Instrumente with a theoretical resolution of 10 nm in closed loop operation. As a CCD we used a monochrome camera model BCN-B013-U from Mightex with a pixel pitch p_x of 5.2 μm. The objective lens, a microscope objective L25/0.22 from Leica, corrected for 160 mm tube length, along with a 160 mm tube caused a magnification of about 25× on the camera. The surface of the aluminum target was preconditioned with fine sandpaper to achieve better statistical properties of the reflected light. This was stipulated by the knowledge that contrast and speckle statistics might change under certain conditions [9]–[11].

Whereas amplitude variations are of minor importance, a polarization stabilized laser has to be used to achieve the highest stability of the speckle field. We used a HeNe laser from Agilent made for interferometer applications (model HP5517A) [12]. Since the laser has two linear orthogonal polarizations, a sheet polarizer from Polaroid (HN32) was applied to ensure stable speckle images by using only one polarization. The setup was highly sensitive to mechanical disturbances. The absence of the experimenter, as well as the improvisatory isolation from air flow, was necessary to obtain reproducibility and precision.

The best results were achieved using specular reflection. The illumination and detection were realized under an angle of approximately 25° to the normal of the plane of diffusion. In most of the measurements, the effective field on the CCD camera was reduced to a resolution of 320×240 pixels. This corresponds to an area of about $66 \mu\text{m} \times 50 \mu\text{m}$ on the object surface. A typical speckle image recorded by the camera can be seen in Figure 4

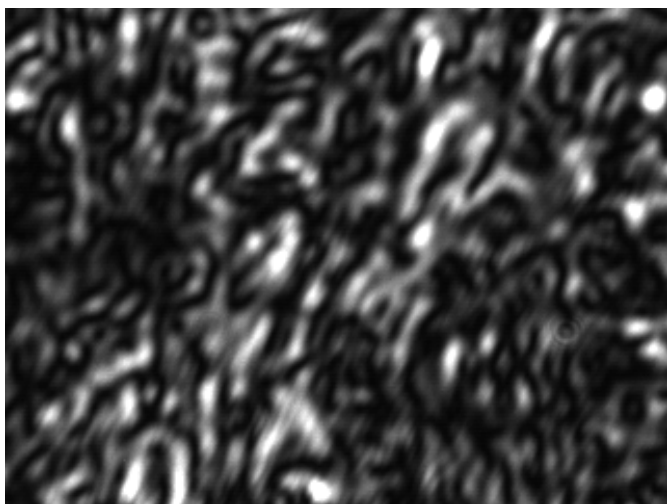


FIG. 4 A typical measured speckle image. Surface conditioning with fine sandpaper was needed to obtain speckle images with good statistical properties.

4 EXPERIMENTAL RESULTS

The setup was prone to some systematic errors like aberrations of the imaging optics and calibration errors of the piezoelectric table. It is very difficult to determine these errors without reference measurements. We followed a more pragmatic approach by studying the repeatability and drift to estimate the relative errors for a defined measurement range rather than qualify the system for absolute distance measurements. Systematic errors could be identified that bear the potential of being corrected in a compact measurement system. We found that the measured results for displacements in the positive direction were systematically linearly shifted compared to the ones in the negative direction. This behavior is unlikely to be caused by piezo calibration problems. A possible reason might be that the cross correlation curves of the speckle images are not symmetric around the zero displacement peak position, which would result in a systematic shift of the peak positions when using a Gaussian bell curve fit. Therefore, left and right movements change the shape of the cross-correlation peak rather than its position. Such effects were not corrected in the measurements allowing better judgment of the quality of the raw data. Since all systematic errors were reproducible with a fixed setup, they could be corrected for a given implementation. So it is convenient to define the error as derivation to some smoothed line that respects a possible calibration error and systematic shifts.

In Figure 5, two examples of measurements for an identical measurement range are shown. The upper panel of the subfigures gives a direct comparison between the measured position values and the position values read at the piezoelectric stage over the full measurement range. The lower panel of each subfigure shows the difference to a linear fit and a confidence band of 10 nm. One can see that the derivation from the linear fit is clearly within the confidence band of ± 10 nm for a range of 50 μm . Furthermore, the shape of the confidence band is unchanged between two different measurements presented in Figure 5. This behavior was reproducible for all measurements. This leads to the conclusion that systematic errors are the main reason of error in the proposed experiment.

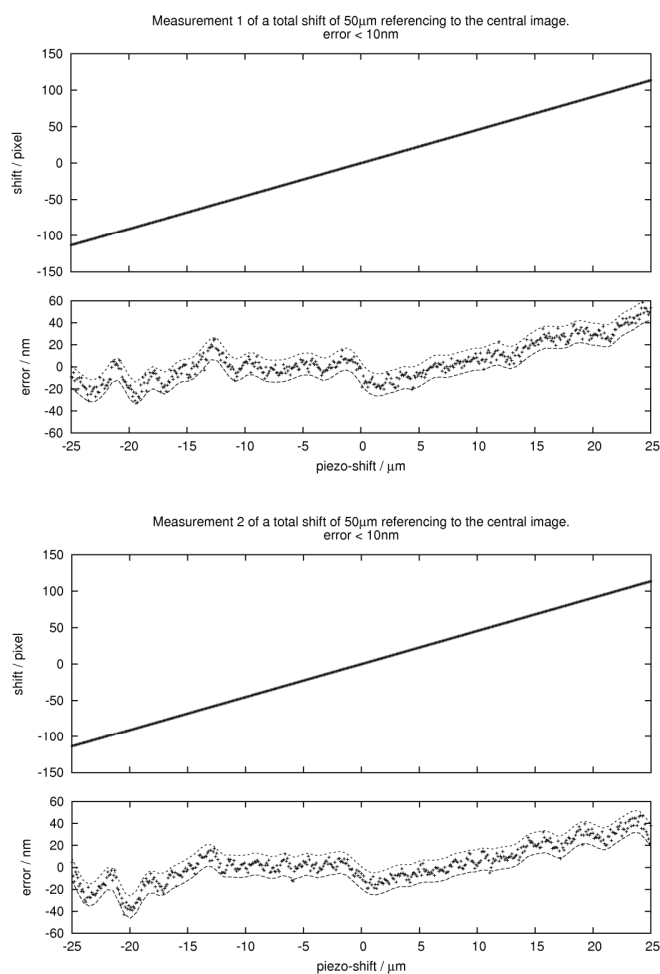


FIG. 5 Two different measurements of displacements for the same measurement range. In the upper part of each subfigure, measurements of shifts compared with the positions given by the piezo-electronics are plotted. In the lower part of the subfigure, deviations from the linear fit are shown. For both cases, the results are within a smoothed confidence band of ± 10 nm. The shape of the confidence band remains nearly unchanged between the measurements. This shows that systematic errors are responsible for the position evaluation.

The extension of the measurement range is one of the most important demands. An approach to extend the range by using a two-image-library is described in [7]. A convincing concept is the stitching of measurements by recording reference speckle images for calibrated positions and measuring the displacement with reference to those images.

As a feasibility test we propose the following measurement. Two reference images are recorded within a distance of good correlation. The positions of test-measurements within this range can then be evaluated with respect to these reference images. If these measurements relative match with sufficiently high precision, the measurement range can be extended by using more reference images. To achieve an absolute measurement scale, only the knowledge of magnification, thus the relation of displacement in pixels with respect to the real displacement, and the absolute position of one reference image has to be known. Hence, this process of building a library of reference images is a self-calibrating process.

As an example, a measurement with two reference images at 0 μm and 25 μm is shown in Figure 6. The extended measure-

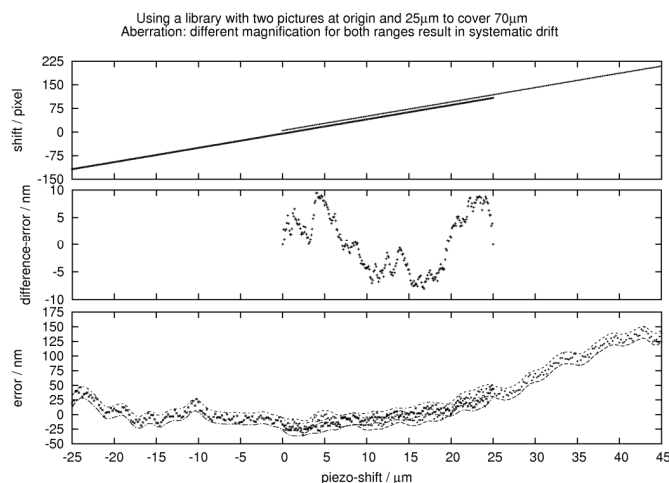


FIG. 6 Test of a library with two reference images at $0 \mu\text{m}$ and $25 \mu\text{m}$ to extend the measurement range up to $70 \mu\text{m}$. Upper diagram: Measured positions compared to the ones given by the piezo-electronics, shifted apart for visibility reasons. Middle diagram: half of the difference between calculations for the two reference images. The absolute value staying under 10 nm is the error of a total measurement in the overlap. Lower diagram shows the calculated positions compared to the linear fit obtained by the $0 \mu\text{m}$ reference image. The linear drift of the second range is caused by aberrations.

ment range is $70 \mu\text{m}$. In the upper part of the figure, the measured positions are compared to the positions indicated by the piezoelectrically driven table. The curves are matching within the error limits, but are shifted apart in the figure for visibility reasons. In the middle of Figure 6, half of the difference between the evaluated positions with respect to the two reference images is shown. In the overlap region, the absolute difference value stays smaller than 10 nm and represents the error of a total measurement. In the lower diagram of Figure 6, the calculated positions are compared to the linear fit obtained with the reference image at $0 \mu\text{m}$. In our measurements, displacements larger than $20 \mu\text{m}$ cause errors in the position evaluation. Aberrations of the optical system lead to magnifications that vary over the field of view of the CCD camera. This results in an increased measurement error for long displacements as the evaluation procedure assumes constant magnification over the whole field of view. Nevertheless, the measured shifts in the overlapping region are highly consistent, confirming the 10 nm accuracy. Using a library with more reference images would give the possibility to further extend the measurement range.

5 DISCUSSION

In speckle displacement measurements, the precision of the displacement evaluation depends on several factors. Aberrations appear when the acquisition of optical signals by imaging under oblique observation is done. Often, a deformation of the speckle field can be observed where the characteristic speckle size varies over the field of view [13]. This is also the case in our measurement system. In general aberrations lead to two effects: decorrelation of the speckle pattern and alteration of the displacement value [14]. Some of the aberrations might be corrected and the sensitivity of the displacement value can be evaluated [15]. In our experiment, we used

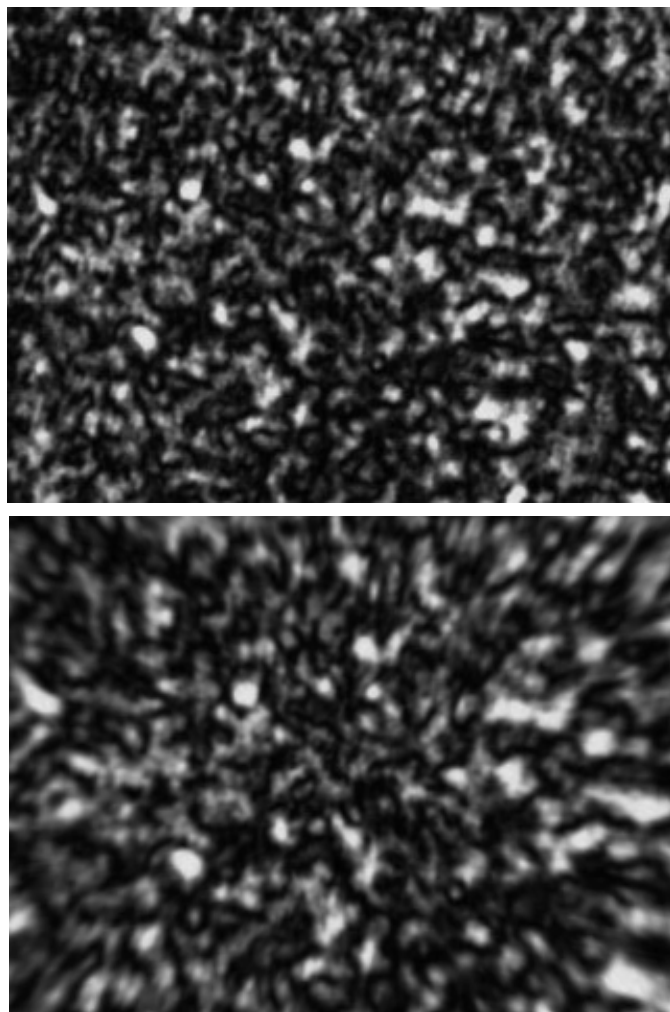


FIG. 7 Change of speckle images subjected to aberrations: top the original and bottom the deformed speckle image that shows image distortions of $s = -40$ and a shift of $d = 30$. The severe distortions lead to a modification of characteristic speckle sizes.

a microscope objective with a high degree of correction in oblique observation. It can be assumed that spherical aberrations, coma and astigmatism are small. We observed nevertheless a difference of the displacement over the field of view, hence varying magnifications, which is typical for distortion. To study the influence of such distortions on the measurement precision, we performed simulations.

An experimental recorded speckle pattern that is subjected to field distortion can be modeled in a simple way by assuming that a recorded image is stretched proportional to its squared distance from the center point. Either the inner parts have a higher magnification than the outer parts leading to a barrel-shaped distortion, or conversely pincushion-shaped distortion. Figure 7 gives an example of a measured speckle image and a corresponding artificially deformed one. The displacement value between images of constant deformation can be evaluated using autocorrelation and averaging as described above. We limit our analysis to field distortion. Computationally, this can be achieved in terms of a two-step coordinate transformation. Step one is simply the translation given by

$$A : (x, y) \rightarrow (x \pm d, y), \quad (2)$$

whereas step two, defined as

$$B : (x, y) \rightarrow (x \cdot (1 + a \cdot r); y \cdot (1 + a \cdot r)) \quad (3)$$

with $r = \sqrt{x^2 + y^2}$, corresponds to the nonlinear deformation where the parameter a sets the degree of distortion. The new image F_n is found using the interpolation of a reference image F_o via

$$F_n(x, y) = F_o(BA(x, y)). \quad (4)$$

Thus, the intensity value initially found at (x, y) is found at a different position afterwards. All directions are equally treated by using the distance from the center as scaling factor.

One can further define a parameter s that gives the deformation on the horizontal axis in terms of pixels,

$$s = \left(\frac{N_x}{2}\right)^2 \cdot a \cdot p_x, \quad (5)$$

where N_x is the resolution of the image in the direction of translation and p_x is the pixel pitch. For $N_x \times N_y = 320 \times 240$ points and a pixel pitch of $p_x = 5.2 \mu\text{m}$, the image size is $1.664 \text{ mm} \times 1.248 \text{ mm}$. An image shift of 1 pixel, thus $s = 1$, leads to a value for the parameter a of $a = 1202 \text{ m}^{-1}$. We evaluated the displacement measurements with values for s of up to ± 50 . This represents a maximal horizontal deformation of 50 pixels, which is enormous. In Figure 8, we show the development of the autocorrelation curves for a shift of $d = 100$ pixels, a shift that corresponds to $520 \mu\text{m}$ in our measurement geometry. Without distortion, the curve has a narrow shape that gets wider and shifted as the distortion is increased, which indicates an increased decorrelation. For $s = -50$ one finds a relative error of about 20%. Small deformations below 5 pixels lead in good approximation to a linear behavior. For a displacement of $d = 100$, one finds for $s = -10$ an evaluated position value of 105, hence 5% deformation. The precision we are aiming on is 10 nm over a maximum measurement range of $50 \mu\text{m}$. This represents an error of 0.02%. Assuming a linear behavior we see that the maximum permitted deformation has to be smaller than $s = 1/25$, a twenty-fifths of a

pixel pitch. Such deformations are at the limit what could be recorded if interpolation between pixels is considered [16].

We predict that the following modifications will improve the precision to better than 5 nm over a range of at least $150 \mu\text{m}$ for the case of one reference image. The peak position of the cross correlations can be calculated more accurately with an approach like the one given in [17]. A modification using Chebyshev polynomials instead of Fourier series might be useful. Cross correlations are normally computed using a fast Fourier transformation. To employ a non equidistant Fourier transformation following [18] will help to correct the known aberrations and distortions. This will also open the possibility to use images with higher resolutions. Using a larger field of view, the correlation can be improved and the accessible measurement range is extended. Furthermore, constraints on the precision of the optical setup can be limited if different optical components are used. Scaling parameters like smaller pixel pitch p_x on the CCD will directly lead to higher accuracy. Today's available cameras reach pixel pitches of $1.2 \mu\text{m}$. The reduction of the pixel size by a factor of three leads in Eq. (4) to three times smaller s values and to a direct increase in precision by the same factor. At the same image field with the same number of points, the field size will be smaller leading to less distortion.

6 CONCLUSION

We have presented a method to measure linear motions using speckle metrology with high accuracy using a new algorithm based on statistical evaluation of one dimensional cross correlation. The method was successfully tested with a rather simple setup. Along with integrated computer hardware, the implementation of an image library will give the possibility to determine absolute positions on long ranges up to several centimeters, which is interesting for industrial applications.

7 ACKNOWLEDGEMENTS

The authors are indebted to Norbert Lindlein for discussions on optical aberrations and acknowledge funding from the CTI (contract ELECTRE 9124.1;5 PFNM-NM).

References

- [1] "Laser Speckle and Related Phenomena" J. C. Dainty, ed. (Springer-Verlag, Berlin Heidelberg New York Tokyo, 1984).
- [2] J. W. Goodman, *Speckle Phenomena in Optics: Theory and Applications* (Roberts and Company Publishers, USA, 2007).
- [3] www.logitech.com, for example model G9x Laser Mouse with 5700dpi.
- [4] For instance model LM13 DP from Renishaw, <http://www.rls.si>.
- [5] For instance LIP 382 from Heidenhain, <http://www.heidenhain.com/>.
- [6] I. Yamaguchi, and T. Fujita, "Linear and rotary encoders using electronic speckle correlation" *Opt. Eng.* **30**, 1862-1868 (1991).

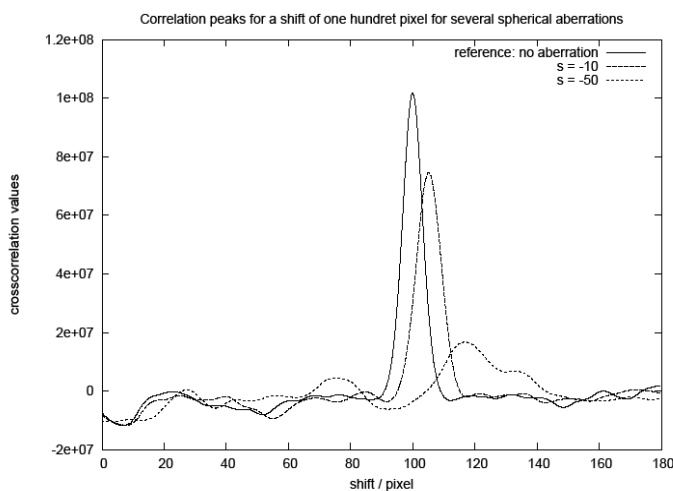


FIG. 8 The auto-correlation evaluated for a shift of 100 pixels for different distortion values of the speckle image. A shift of the peaks marks the severe error on the measurement for large distortions. At the same time decorrelation happens and leads to broader peaks resulting finally in a shortening of the measurement range.

- [7] V. Shilpiekandula, *A laser speckle based position sensing technique* (Master's thesis, Massachusetts Institute of Technology, 2004).
- [8] W. Wang, T. Yokozeki, R. Ishijima, M. Takeda, and S. G. Hanson, "Optical vortex metrology based on the core structures of phase singularities in Laguerre-Gauss transform of a speckle pattern" *Opt. Express* **14**, 10195-10206 (2006).
- [9] H. M. Pedersen, "The roughness dependence of partially developed monochromatic speckle patterns" *Opt. Commun.* **12**, 156-159 (1974).
- [10] J. W. Goodman, "Dependence of speckle image contrast on surface roughness" *Opt. Commun.* **14**, 324-327 (1975).
- [11] R. D. Bahuguna, K. K. Gupta, and K. Singh, "Speckle patterns of weak diffusers: effect of spherical aberration" *Appl. Opt.* **19**, 1874-1878 (1980).
- [12] Technical Support:5517A Laser Head, <http://www.home.agilent.com>.
- [13] R. D. Bahuguna, K. K. Gupta, and K. Singh, "Study of laser speckles in the presence of spherical aberration" *J. Opt. Soc. Am.* **69**, 877-882 (1979).
- [14] L. Martí-López, "Effect of primary aberrations on transverse displacement of laser speckle patterns" *Opt. Laser Technol.* **28**, 15-19 (1996).
- [15] L. Martí-López, and O. Mendoza-Yero, "Effect of compensation for spherical aberration on the transverse displacement of laser speckle patterns" *J. Opt. Soc. Am. A* **17**, 1407-1412 (2000).
- [16] N. Schuster, "Messen mit Subpixel-Genauigkeit" in *Optik & Photonik* **3** 49-52 (Wiley-VCH Verlag, Weinheim, 2007).
- [17] T. Roesgen, "Optimal subpixel interpolation in particle image velocimetry" *Exp. Fluids* **35**, 252-256 (2003).
- [18] S. Kunis, J. Keiner, and D. Potts, "Using NFFT 3 - a software library for various nonequispaced fast Fourier transforms" *ACM T. Math. Software* **36**, 1-30 (2009).